Resolving temporal threat uncertainty by observational learning involves the amygdala, hippocampus and anterior insula

Temporal uncertainty in observational learning

Simon Knobloch[a]*, Theresa, Jansen[a], Lara Hille[a], Madeleine Müller[a,b], Leonie Rumpf[a], Jan Haaker[a]

[a] Department of Systems Neuroscience, University Medical Center Hamburg-Eppendorf, 20246 Hamburg, Germany.

[b] Department of General Psychology and Cognitive Neuroscience, Charlotte Fresenius University, 20148 Hamburg, Germany

*Corresponding author. Email address: simon.knobloch@rwth-aachen.de

This manuscript is currently under review at the 'Journal of Neuroscience'.

Abstract

While the neurobiological distinction between temporally predictable (cued) and unpredictable (contextual) threats has been well-characterized in direct learning using the NPU paradigm, it is poorly understood how these processes unfold during observational learning, a key mechanism of human threat-learning. In this study, we developed a novel observational paradigm based on the NPU paradigm (Experiment 1, n=20, male and female) and combined it with fMRI (Experiment 2, n=23, male and female) to investigate how the brain encodes predictable and unpredictable threat cues observed in others. Participants learned predictable (P), unpredictable (U), and no-threat (N) cues by observation and encountered the same threat cues during an expression phase. Threat expectations indicated that participants successfully learned threat contingencies, showing heightened threat expectations for predictable cues and unpredictable contexts. This converged with neural responses in the anterior insula during the expression phase. Reflecting the dynamic process of learning, the amygdala responded to predictable threat cues with a linear decrease across trials. Interestingly, we found that learning to predict threats from others' pain was accompanied by enhanced neural response within the amygdala, insula and hippocampus, as compared to unpredictable conditions. Our findings suggest that humans learn to resolve temporal uncertainty relying solely on observation. The ability to learn shapes the neural response to an observed threat.

1. Introduction

Accurate prediction of threats is key to survival. Since we live embedded in sociocultural surroundings, observational threat learning enables us to predict dangers without any direct encounter of threats (Berger, 1962; Vaughan and Lanzetta, 1980; Olsson and Phelps, 2004). In observational fear learning it has been shown that the demonstrator's expression of pain serves as an unconditioned aversive stimulus that enables to learn a predictive threat cue, which was conditional for the response observed in the demonstrator (Olsson et al., 2007). The learning processes closely mirror firsthand threat learning both in behavioral fear reaction and neural response (Olsson et al., 2007; Haaker et al., 2017a; Lindstrom et al., 2018; Olsson et al., 2020). Specifically, the amygdala has been shown to play a central role in direct learning (Quirk et al., 1995; Buchel et al., 1998a; Buchel et al., 1998b; Marschner et al., 2008) and observational learning (Olsson et al., 2007; Haaker et al., 2017a). As a crucial difference between observational and direct learning, it has been noted, that in social learning the anterior insula, rather than the amygdala plays the central role in relaying the input of the observed unconditioned stimulus to a neural network for aversive learning (Lindstrom et al., 2018). This knowledge led to the development of experimental paradigms to capture the mechanisms of acquired fear through observation (Olsson et al., 2007; Haaker et al., 2017b). However, these paradigms commonly used temporally predictable threats. Yet, from a functional perspective, humans have to be able to resolve information that indicate threatening contexts or situations, in which threats occur unpredictably (Blanchard et al., 1993; Davis et al., 2010; Schmitz and Grillon, 2012).

Regarding the distinction of predictable threat cues and context-related sustained threat, the NPU-paradigm (no-pain, predictable pain and unpredictable pain) has been developed to model responses comparable to the dissociable defense mechanisms of fear and anxiety (Schmitz and Grillon, 2012). Participants learn to discriminate the three conditions and develop dissociable reactions to the three conditions, with an elevated anxious arousal (e.g., measured by startle-responses) towards the predictable cue and the unpredictable context (Alvarez et al., 2011; Schmitz and Grillon, 2012). Neurally, a differential contribution of the amygdala to predictable threat learning (Marschner et al., 2008; Alvarez et al., 2011; Shankman et al., 2014; Naaz et al., 2019) and the hippocampus (Alvarez et al., 2008; Marschner et al., 2008) to uncertain threat learning has been proposed to be a central discerning feature of the two threat types. It has to be noted though that the amygdala has also been shown to be involved in contextual (i.e. unpredictable) threat conditioning (Alvarez et

al., 2008; Figel et al., 2019). The insular cortex, apart from the mentioned role in observational learning, has been shown to be involved in the anticipation of uncertain threats (Alvarez et al., 2011; Shankman et al., 2014; Herrmann et al., 2016; Geng et al., 2018; Hur et al., 2020; Radoman et al., 2021).

In our study, we aimed to examine the acquisition of predictable threat cues and sustained responses to unpredictable threats by social means. To this end, we developed a novel paradigm, in which participants observe a demonstrator encountering threat (delivered through painful stimulation) in an NPU-based design. The cued pain occurrence can be learned to be resolved in the predictable condition but is temporally unresolvable in the unpredictable condition. We hypothesized (in Experiment 1) that participants will be able to resolve the threat-related information by observation and show discriminable threat expectations to predictable and unpredictable cues and contexts when confronted directly in the expression phase. We pre-registered our hypotheses in Experiment 2 that neural responses in the amygdala, hippocampus and insular cortex underlie learning from others' pain to resolve temporal predictability.

2. Methods

2. NPU paradigm

Conceptual basis of the experimental paradigm developed for this study was the NPU paradigm that includes firsthand experiences of an unpleasant electrotactile stimulation to induce a threat (Schmitz and Grillon, 2012). Our study adapted this protocol to examine observational learning within a predictable pain condition [P], unpredictable pain condition [U] and no pain condition [N]. Conceptual basis for our observational learning paradigm is a well-known two-phase experimental paradigm, in which participants learn threat/cue contingencies by observation in stage one (observation phase), and in stage two (expression phase) directly encounter the cues learned to predict threat or safety (Haaker et al., 2017b).

We report two experiments in this publication. In Experiment 1 we developed and tested the observational learning paradigm in the behavioral lab. In Experiment 2 we adapted the paradigm for use in fMRI. We, thus, were able to retest preregistered behavioral results from Experiment 1 in an independent sample in Experiment 2 and advance the understanding of the underlying mechanisms through the analysis of neural correlates. The conducted analyses were preregistered prior to data-analysis (Knobloch et al., 2024).

2.2 Experiment 1

2.2.1 Participants and procedure

20 healthy participants (age-range: 18-40) were recruited by online and black-board postings at the University Medical Center Hamburg. All participants were fluent in German and able to understand the task instructions. Exclusion criteria were current or previous psychiatric disorder, current use of psychoactive medication or substances and current or previous neurological disease. Participants that had already participated in threat-conditioning studies at our institute within three months preceding the participation were also excluded. Eligibility criteria were assessed in structured interviews via telephone and verified on site by a physician. Study data was collected in a single appointment of approximately 90 minutes. After giving informed consent to participate in the study, participants filled out a questionnaire collecting sociodemographic data.

The experiment consisted of two blocks of 25 minutes (see 2.2.3 Experimental Design) and was conducted on a computer in the behavioral lab. After completing the experimental paradigm participants filled in a post-experimental questionnaire, in which they answered questions about the cue/pain contingencies and rated the observed pain expression with regard

to naturality and their empathy towards the demonstrator. All questionnaires were conducted via soSci (soscisurvey.de, München, Germany).

Study procedures were in line with the Declaration of Helsinki. The ethics committee of the Hamburg medical chamber approved the study. Participants that finished the study received an expense compensation of 15€.

2.2.2 Stimuli

33 Videoclips for P and U with randomized pain onset and -duration were recorded. The videos show a demonstrator model who is watching a screen and receives painful heat-stimulation. The demonstrator wears a cuff around his right upper arm (see Fig 1 a) and the heat stimulation device (via a thermode) is placed under the cuff. The response of the demonstrator to the heat stimulation reflected the painful experience. In order to choose video clips for the experiment that were comparable in pain expression, two independent individuals rated five components of the demonstrator's pain expression: lip press, head protrusion, eye closure, forehead wrinkle and masseter contraction. Additionally, three individuals rated independently the binary presence of the five components as well as pain visibility duration (in seconds) and pain-intensity (scale from 1-10). All clips that featured at least four pain components (marked as present by at least one of the three reviewers) entered a propensity-score based matching. Propensity score was calculated by the mean rated pain-intensity and duration. The caliper width of the matching was reduced until a subset of 12 clips for each condition remained for Experiment 1. The 12 included clips did not differ significantly in pain-intensity ($p = .690$) and visible pain duration ($p = .918$) in Experiment 1.

2.2.3 Experimental design

The experiment was divided into two phases: observation-phase and expression-phase.

In the observation-phase participants were instructed to watch videoclips of a novel blood-pressure measurement approach, which was highly precise yet painful. They were told to watch the patient's pain-expression as well as the screen, visible in the video. The screen in the video showed three grey bars stacked vertically. Each bar had a colored portion of different size and position and a black slider at the left-hand side of the bar. Depending on the experimental condition, one of those sliders started moving from the left-hand side of the grey bar to the right. In P, the slider crossing the colored part of the bar predicted the pain expression of the demonstrator. In U, the slider position had no predictive value for the demonstrator, i.e. the demonstrator's pain responses were visible at random slider positions in

each video clip. In N no pain expression was visible (see figure 1 a for an overview of slider/pain relation). Each video-clip lasted from the moment the slider started moving till it reaching its final position on the right-hand side of the grey bar (24s). Participants were asked to rate the pain intensity for each clip. In total participants completed 12 trials in each condition.

In the second phase, the expression-phase, participants were directly confronted bar setup, that was previously visible on the demonstrator's screen.(as depicted in Fig 1 b)). Similarly, the clips lasted from the moment the slider started moving till it reached its final position on the right-hand side of the grey bar. Participants were asked to answer questions regarding their expectations about painful stimulation in each clip and did not expect to receive painful stimulation themselves. In total participants completed 12 trials in each condition.

2.2.4 Ratings

During the observation phase, participants were asked to rate the observed pain intensity on a scale generating values from 1-100 (1 = no pain, 100 = strong pain). The rating query appeared during the pain-expression of the demonstrator. For the rating, the video-clip was paused and blurred. In the N condition, the participants rated the same question while no pain was visible.

During the expression phase, participants were asked to rate their threat expectation and certainty at three locations of the moving slider (context-expectation: slider position 2,5 seconds before the colored part of the bar, cue-expectation: slider position in the middle of the colored part of the bar, safety rating: slider position 2.5 seconds after the colored part of the bar). Note that due to a technical error in the script the first four participants were not asked for safety ratings (safety rating n = 16). Answers were given on a scale generating values from -100 (certainly no pain) via 0 (uncertain) to 100 (certainly pain). For each expectation-query, participants were asked to rate both an expectation for the demonstrator confronted with that screen setup and a self-rating when picturing themselves being confronted with the screen setup.

All answers were generated by using the arrow-keys of a standard keyboard.

2.3 Experiment 2

2.3.1 Participants and procedure

Based on the pilot study (N=20), the relevant interaction yielded an effect size of partial eta squared = 0.331, which results in a power of >99% for 20 participants. Thus, we determined the sample here to be 25 participants including dropouts. Thus, 25 healthy participants (age-range: 18-40) were recruited by online and black-board postings at the University Medical Center Hamburg. Eligibility criteria were equal to Experiment 1. Additionally, participants unable to undergo fMRI scanning due to ferromagnetic or electrical implants as well as unspecified foreign bodies were excluded from the study-participation.

Study data was collected in a single appointment of approximately 120 minutes. The procedure was similar to Experiment 1 except for Experiment 2 being conducted in the fMRI scanner. In Experiment 2 skin-conductance-reading [SCR] were collected to assess the psychophysiological response. Furthermore, in Experiment 2 participants filled out the State-Trait Anxiety Index [STAI] (Spielberger et al., 1970) and the Affective and Cognitive Measure of Empathy [ACME] (Vachon and Lynam, 2016).

Neuroimaging acquisition consisted of two functional imaging blocks, each taking approximately 25 minutes (observation and expression, see 2.3.3 Experimental Design). Subsequently a T1 weighted image (ca. 5 min.) for co-registration and a T2 weighted image (ca. 10 min.) were collected. The data from the T2 weighted image is not reported in this study.

2.3.2 Stimuli

For Experiment 2, caliper width was further reduced to reduce the subset to 10 video clips. The 10 included clips did not differ significantly in pain-intensity (p= .612) and visible pain duration (p= .912) in both subsets respectively. One clip of P and U respectively, matched in pain-intensity and -duration was chosen and used thrice for the three rating trials. The other 9 trials were used once each for the non-rating trials.

2.3.3 Experimental design

The two-phase experimental design did not differ from Experiment 1. In Experiment 2 participants rated pain intensity in the observation phase and threat expectations only in three of the twelve trials. The other nine trials ran without rating interruption for the analysis of neural correlates.

In the expression-phase participants wore an identical cuff around their right upper arm as seen on the demonstrator and were told that it might inflict some unpleasant yet not highly painful stimulation in Experiment 2. As in the observation-phase, participants rated only one identical trial three times. The remaining 9 trials ran without rating interruption. Furthermore, participants completed one rating trial of the expression-phase before the observation phase to collect expectations without relation to the information learned in the observation-phase.

2.3.4 Ratings

All answers were collected by using a 4-button box. The scales used in Experiment 2 were identical to the ones from Experiment 1. In the expression-phase, participants were only asked to rate threat expectation and certainty regarding themselves being in the same situation as the demonstrator before. No expectations about the demonstrator were collected.

2.3.5 Image acquisition

All images were acquired using a 3 Tesla Siemens Prisma scanner (Siemens AG; München, Germany) at the Institute for Systems Neuroscience at the University Medical Center Hamburg-Eppendorf. For this study, echo-planar imaging sequences sensitive to blood oxygenation level-dependent changes were acquired for the functional analysis. 52 axial slices of 1.5mmx1.5mmx1.5mm voxels were acquired (TR = 1848ms, TE = 30ms, flipangle = 70°). Subsequently, an anatomical image was acquired (T1 weighted 3d image, magnetization prepared rapid acquisition gradient echo image, 1 mm x 1mm x 1mm voxel size, TR = 7.1 ms, TE = 2.98 ms, TI = 1100 ms, matrix = 256 × 256, 240 slices, flip angle = 9°).

2.3.6 SCR

Skin-Conductance was collected using two palmar electrodes of the participants left hand. Spike2 software (Cambridge Electronic Design Limited, Cambridge, England, RRID:SCR_000903) was used for data collection. MRI-pulses were collected to synchronize the experiment's logfiles.

2.4 Statistical analysis

2.4.1 Behavioral analysis

In both Experiments (1&2) mean threat expectation ratings from the expression phase were analyzed in a 3x2 repeated measurement ANOVA with condition (P, U, N) and cue/context (cue-expectation, context-expectation) as factors. For post-hoc comparison that would

characterize an interaction between condition and cue vs. context, the cue-prominence was calculated for all conditions separately by subtraction of the context-expectation from the cue-expectation. Cue prominence was compared among the conditions in paired-sample t-tests (P vs. N, U vs. N, P vs. U). In Experiment 1 a similar repeated measurement ANOVA and post-hoc t-tests were calculated for expectation of pain for the actor. To account for beliefs held by participants unrelated to the observable predictability of the conditions, we report pre-observation ratings for threat expectation and compare them similarly across conditions in Experiment 2. Safety-ratings (slider-position behind colored part of the bar) were compared in a 1x3 repeated measurement ANOVA among the conditions in both Experiment 1 and 2. Significant effects were followed up using paired-sample t-tests. Furthermore, mean pain ratings from the observation phase were compared among the pain-conditions in a paired-sample t-test (P vs. U).

Level of significance was set to $p < .05$. Multiple comparisons were accounted for through Bonferroni-Holms correction. All statistical analyses were conducted using JASP 0.18.3.0 (RRID:SCR_015823). Matlab 2023b (Mathworks Inc., Natick, Massachusetts, USA, RRID:SCR_001622) was used to read-out logfiles and count the participants' answers.

2.4.2 fMRI analysis

Participants were checked for excessive movement prior to analysis (preregistered exclusion criterium = 3x voxel-size lead to deletion of affected volumes, participants exceeding 25% data quality issues were excluded from analysis). In both experimental phases of Experiment 2 (observation and expression) cue and context regressors were modelled following the focus of the behavioral analysis of cue- and context-expectation. To prevent cue-, context- and pain-regressors from being colinear, cue-onset-regressors were modelled as event regressors at the onset of slider movement and cue regressors as event regressors in the moment the slider started the passage of the colored part of the bar. Pain-regressors were modelled as event-regressors at the onset of pain-expression, as rated by three lab members for each video clip. For N, whose stimulus videos did not contain visible pain in the demonstrator, a no-pain event regressor was modeled starting approximately (in a random interval) 2s after the cue-regressor. A box-car regressor was modelled for the whole 24 s of each videoclip representing sustained context activations through the experimental condition. ITI, instructions and ratings were modeled as separate box-car regressors. Regressors were convolved with the

hemodynamic response function in the first level analysis. Temporal autocorrelations were accounted for through AR1.

For the second-level analysis a one-factor (3 levels: experimental condition) full factorial design was calculated for each regressor separately: cue, context-onset and context both in observation and the expression phase, as well as pain during the observation phase. Furthermore, a two-factor full-factorial design with one factor comprising cue and context and the other factor the three experimental conditions was applied to analyze neural substrates of cue-prominence. We report the following t-contrasts for the one-factor analyses: P>N, U>N, P>U, U>P. For the cue-prominence analyses, we report an interaction contrast with cue >context-onset in P and cue < context-onset in U. For the analysis of pain related activation, we report a secondary t-contrast P&U>N for the analysis of neural correlates of pain-expression in general. In a subsequent analysis (following Marschner and colleagues' analysis (2008), the same first-level regressors were used with linear time-modification over the course of the trials. We report the contrast P>U (i.e. increasing activation in P and decreasing activation in U) and U>P (i.e. vv.).

For all analyses we report activation of 3 predefined ROIs (right and left separately): amygdala, hippocampus, insular cortex from the Harvard - Oxford Cortical Structural Atlas (RRID:SCR_001476). Clusters that surpass peak-voxel FWE correction at $p<.05$ in small volume correction (across all 6 ROIs) are reported. SPM25 (RRID:SCR_007037) was used for the analysis of the fMRI data.

2.4.3 SCR analysis

The collected SCR data from the experiment was analyzed using PSPM7.0. Raw data was trimmed from the onset of the first non-rating trials till the last MRI-pulse of the two experimental phases separately. Trimmed data was assessed visually for data quality. Participants with at least 50% noisy- or zero-line data were excluded from further analysis. Regressors for context onsets, cue onsets (and pain onsets in the observation phase) were modeled and convolved with the canonical skin conductance response function. Following the design of the behavioral analysis, a 2x3 repeated measurement ANOVA with condition (3 levels) and cue/context (2 levels) as factors are reported. Significant factors were followed up using paired-sample t-tests. Pain related skin-conductance alterations were compared using paired-sample t-tests among the three conditions.

3. Results

3.1 Sample characteristics

In Experiment 1, the 20 recruited participants all entered the analysis. A description of the study sample can be found in Table 1.

In Experiment 2, 25 participants were recruited. One was excluded due to technical problems with stimulus presentation and erroneous data collection. A second participant was excluded, due to excessive movement during acquisition preventing the generation of a clean T1 image for coregistration. A description of the remaining sample of 23 participants can be found in Table 2.

3.2. Behavioral results

3.2.2 Experiment 1

First, we tested the central hypothesis that participants learn the temporal predictability of cues the aversive outcomes by observation. To this end, we tested participants' threat expectation for firsthand outcomes in P vs. U in the expression phase. Indeed, the repeated-measurement ANOVA of rated threat expectation revealed a significant influence of the condition ($F = 15.175$, $df = 2$, $p < .001$), cue/context ($F = 62.033$, $df = 1$, $p < .001$) and their interaction ($F = 9.383$, $df =2$, $p < .001$) (see Table 3). Post-hoc t-tests to follow upon this interaction compared cue and context expectation, i.e., 'cue-prominence' (cue-expectation – context-expectation) between conditions thus revealed higher cue-related expectation in P ($t= 3.994$, $df = 19$, $p = 0.00078$, p Holm = 0.00234) and U ($t= 2.449$, $df = 19$, $p = 0.024$, p Holm = 0.048) as compared to N. The comparison of the cue-prominence between P and U revealed a trend of a higher cue-prominence in P ($t= 1.997$, $df = 19$, $p = 0.06$, p Holm = 0.06). Table 4 and Table 5 give an overview of the behavioral outcome measures and the statistical analyses. Raincloud plots of the expectation results can be found in Figure 1b).

We additionally asked for participants expectation about the pain that the demonstrator might receive during the expression phase, which did not match the learned threat contingencies from the observation phase. A 3x2 repeated measurement ANOVA revealed a significant influence of the condition ($F = 26.685$, $df = 2$, $p < .001$), cue/context ($F = 14.936$, $df = 1$, $p < .001$) and their interaction ($F = 8.325$, $df =2$, $p < .001$). Post-hoc t-tests of that interaction showed an increased cue-prominence in both U ($t= 4.751$, $df = 19$, $p = 0.00014$, p Holm = 0.00042) and N ($t= 3.434$, $df = 19$, $p = 0.003$, p Holm = 0.006) as compared to P.

In order to test if threat expectation were sustained, we compared threat expectation after the cursor passed the colored cue, across the conditions, which however only revealed a trend-

wise effect (F = 2.772, df = 2, p =0.079). Descriptively participants rated the lowest threat expectation for N (mean ± SD: -0.82 ± 0.31), a medium threat expectation for P (mean ± SD: -0.66 ± 0.30) and the highest expectation for U (mean ± SD: -0.53 ± 0.43).
Participants furthermore rated trend-wise higher pain-intensity for the demonstrator in P as compared to U (t= 1.910 df = 19, p = 0.071).

3.2.2 Experiment 2

In Experiment 2 we were able to reproduce and advance the results from Experiment 1. Similar to Experiment 1, the repeated measurement ANOVA of threat expectation in the expression phase revealed a significant main effect of condition (F = 22.642, df = 2, p < .001), cue/context (F = 32.291, df = 1, p < .001) and their interaction (F = 13.158, df =2 , p < .001) (see Table 6). Pre-registered post-hoc comparisons again revealed that the cue-prominence increased in P (t= 4.443, df = 22, p = 0.0002, p Holm = 0.0006) and U (t= 2.814, df = 22, p = 0.01, p Holm = 0.02) in comparison to N and we found an increased cue-prominence in P as compared to U (t= 2.808, df = 22, p = 0.01, p Holm = 0.01) (see Table 7 & 8). Rain cloud plots of the mean threat expectation after learning before an at the cue can be found in figure 1 b). The plots illustrate a comparable threat expectation at the cue in P and U, but an increased contextual threat expectation in U as compared to P (Cue-Expectation P vs. U: t = 0.891, df = 22, p = .382, p Holm = .382; Context-Expectation = P vs. U: t = -2.615, df = 22, p = . 016, p Holm = .032). Before learning the threat contingencies in the observation-phase threat expectations were not significantly different (see Table 9).
Participants furthermore sustained a differential threat expectation across conditions after the cursor passed the colored cue (F = 5.989, df = 2, p = .005). We found an increased rating for both P (t= 3.941, df = 22, p = .00066, p Holm = .002) and U (t= 2.581, df = 22, p = 0.017, p Holm = .034) as compared to N. No difference was revealed between P and U (t= 0.313, df = 22, p = .758, p Holm = .758), which might indicate that the predictable condition was evaluated as potentially dangerous, even when the predictable danger signal passed.
In contrast to our pre-registered hypothesis, we found no difference in ratings for the demonstrator's inferred pain between P and U (t= 1.384, df = 22, p = .180).

3.3 fMRI results

3.3.1 Observation phase

In line with meta-analytic evidence (Lamm et al., 2011; Jauniaux et al., 2019) we found that the observation of pain across P and U elicited activation in the left insula (t = 5.93, df =

[1,66], MNI = [-36, 18.5, 0.5], p(FWE) = 0.00006) and amygdala (t = 4.54, df = [1,66], MNI = [-28.5, 0.5, -22], p(FWE) = 0.0031)
(see Figure 2 a) – f)), when compared to no observed pain (i.e., same timepoint in the neutral condition; P&U >N). Observation of predictable pain (P>U) was further encompassed by higher parameter estimates in the right hippocampus (t = 4.27, df = [1,66], MNI = [33, -32.5, -10], p(FWE) = 0.0145), when compared to observed pain that was unpredictable (see Figure 2 g) – i)).

Next, we tested for neural activation that reflects the participant`s ability to distinguish between cue and context-onset in different conditions of temporal predictability. Specifically, we contrasted (pre-registered) hemodynamic responses reflecting cue prominence (P: Cue > Context; U: Context > Cue) between P and U, that mirror participants rated higher cue prominence for P, as compared U (in the expression phase). This contrast only revealed a cluster trending towards FWE-corrected significance in the left (anterior) hippocampus (t = 3.66, df = [1,132], MNI = [-21, -20.5, -20.5], p(FWE) = 0.056) (see Figure 5 a) – c)).
To examine only cue-related activation, we contrasted activation between predictable cues of observed pain, as compared to neutral cues (P > N), which revealed activation in the posterior part of the left hippocampus (t = 3.90, df = [1,66], MNI = [-13.5, -38.5, 2], p(FWE) = 0.041) (see Figure 4). No differences in activation in our ROIs emerged in the comparison of predictable and unpredictable cues (P > U), albeit differences in linearly changing responses to threat cues (see 3.3.3).
When comparing the context-onset related activation, we found higher activation in the left anterior insula (t = 4.51, df = [1,66], MNI = [-36, 11, -14.5], p(FWE) = 0.007) in the unpredictable condition as compared to the neutral condition (U > N) (see Figure 3 a) -c)).
We found no differences in activation in the ROIs at context-onset between U and P. When we examined sustained activation that would last across the whole observational trial, we compared our contrast revealed sustained activation of the right amygdala (t = 3.77, df = [1,66], MNI = [21, -4, -20.5], p(FWE) = 0.027; t = 3.69, df = [1,66], MNI = [30, -4, -16], p(FWE) = 0.034) during the unpredictable threat condition, as compared to the predictable condition (U > P) (see Figure 3 d) -f)).

3.3.2 Expression phase

The neural activation during the expression phase was thought to reflect participant's responses to socially shaped threat expectation that is higher for the cue (as compared to the

context) in the predictable, as compared to the unpredictable condition (i.e., cue-prominence). This preregistered interaction contrast between cues and context-onsets in P and U reflecting the participants' threat expectations (P: cue > context-onset, U: context-onset > cue) revealed a cluster in the right insula (t = 4.23, df = [1,132], MNI = [34.5, 20, 2], p(FWE) = 0.009) (see Figure 5 d) – f)).

Against our preregistered hypothesis, the exposition to mean responses to predictable threat-cues lead to no activation in the predefined ROIs. The comparison between unpredictable cues to predictable cues (U > P) revealed activation in the left hippocampus (t = 5.39, df = [1,66], MNI = [-19.5, -10, -23.5], p(FWE) = 0.0004). We neither found activation in the ROIs at context-onset nor sustained contextual activation.

3.3.3 Linearly changing responses

In order to account for the changes (e.g., extinction) in threat-contingencies during observational learning (i.e., learning from observed outcomes) and direct expression phase (i.e., no firsthand outcomes), we modelled linearly changing activity across trials, focusing on differences between the predictable and unpredictable condition, as preregistered.

The interaction-contrasts related to cue-prominence (contrast: linear decrease cue: P > U; linear decrease context U> P) examined decreasing responses across learning to more valid threat predictors, i.e. predictable cues and unpredictable contexts (see Marschner et al., 2008). During observation, the right insula (t = 3.76, df = [1,132], MNI = [45, 6.5, -7], p(FWE) = 0.045) reflected activation to predictable cues and unpredictable context-onsets that decreased across learning, while activity to unpredictable cues and predictable context-onsets was sustained or increased (see Figure 7 a) – c)). Similarly, the activation in the bilateral amygdalae (t = 4.21, df = [1,66], MNI = [-18, -7, -13], p(FWE) = 0.009; t = 3.97, df = [1,66], MNI = [21, -5.5, -13], p(FWE) = 0.018) (see Figure 6 a) – c)) decreased linearly across trials during observational learning of predictable cues as compared to sustained activity to unpredictable threat cues (contrast: linear decrease P > U), which might reflect an early integration of socially derived threat information in the predictable condition.

In the expression phase, a similar pattern emerged in the right amygdala (t = 4.56, df = [1,132], MNI = [24, -8.5, -14.5], p(FWE) = 0.00013) for the cue-prominence interaction contrast (contrast: linear decrease cue: P > U; linear decrease context U> P), again with decreasing activation to predictable cues (as compared to predictable contexts) and unpredictable contexts (as compared to unpredictable cues) (see Figure 7 d) – f)). In line with

these results is transient right amygdala (t = 3.75, df = [1,66], MNI = [25.5, -8.5, -13], p(FWE) = 0.029) activation to predictable cues in the expression phase (see Figure 6 d) – f)) as compared to increasing responses to unpredictable threat cues, which probably is also driven by the extinction of socially learned contingencies when firsthand outcomes are lacking.

Interestingly, we found that contextual activation in the hippocampus (t = 3.94, df = [1,66], MNI = [-24, -10, -28], p(FWE) = 0.032)was sustained across trials in the unpredictable condition during the expression phase as compared to the predictable condition (contrast: linear decrease P > U) (see Figure 6 g) – i)).

3.4. SCR-Analysis

13 subjects were included into the analysis after data-quality assessment in the observation phase. Only the factor cue/context significantly influenced SCR (F = 17.309, df = 1, p = .001) but not condition (F = 1.438, df = 2, p = .257) or the interaction of condition and cue/context (F = 0.631, df = 2, p = .541). A post-hoc test revealed an increased response to context onsets as compared to cues among all conditions (t = 4.16, df = 12, p = 0.001). Only a descriptive difference (P (mean ± SD) = 0.401 ± 0.948; U (mean ± SD) = 0.195 ± 0.794; N (mean ± SD) = 0.197 ± 0.934) among the responses to predictable pain as compared to both unpredictable (t = 0.896, df = 12, p = .388) and no pain (t = 0.067, df = 12, p = .516) was revealed.
In the expression phase 15 subjects were included after data-quality assessment. No significant effect or interaction-effect of condition or cue/context SCR was found (condition: F = 2.285, df = 2, p = .120; cue/context: F = 3.891, df = 1, p = .069; conditionXcue/context: F = 20.083, df = 2, p = .921).

4. Discussion

Our results show that participants learned to resolve temporal threat uncertainties by observing painful experience in others to predicable cues and unpredictable context-onset. The analysis of neural activations revealed that the left hippocampus was activated during learning from observation. Mirroring the temporally dynamics of learning, we generally found decreasing activation to signals that were learned as valid predictors of threats: i.e., bilateral amygdala activity decreased to predictable cues during observational learning, whereas responses increased to unpredictable cues across trials. In uncertain learning situation sustained hippocampus activation was found across trials. Interestingly, we found that neural responses with key regions for observed pain, the amygdala and insula (Lamm et al., 2011; Jauniaux et al., 2019) were enhanced when the observation of pain could be used for learning to resolve temporal unpredictability (i.e., predictable threat cues), as compared to observed pain that was temporally unpredictable i.e., not learning relevant.

A differential contribution of the amygdala to cued threat learning, i.e. fear (Marschner et al., 2008; Naaz et al., 2019), and the hippocampus (Marschner et al., 2008; Alvarez et al., 2011) to uncertain threat learning has been proposed to discern fear and anxiety neurobiologically. Furthermore, the role of the insular cortex in uncertain threat anticipation has been highlighted in studies that employed both, temporally predictable and unpredictable conditions (Alvarez et al., 2011; Herrmann et al., 2016; Geng et al., 2018; Radoman et al., 2021). Following studies have uncovered a less clear pattern of differentiation, though (Andreatta et al., 2015; Herrmann et al., 2016; Figel et al., 2019; Hur et al., 2020). Our data does not fully support a clear mechanistic separation between brain regions. We found the right amygdala to be sustainedly activated during observation of unpredictable threats. The amygdala has been reported to react phasically to threat cues (Alvarez et al., 2011; Naaz et al., 2019) or unpredictable context onsets (Herrmann et al., 2016; Figel et al., 2019) and threat confrontation (Siminski et al., 2021), in paradigms with firsthand aversive experiences. However, sustained activation of the amygdala during unpredictable threat-contexts has been described to firsthand electric shocks (Andreatta et al., 2015). Interestingly, connectivity analysis supports the view of a contribution of the amygdala towards the resolving of unpredictable threat contexts (Wheelock et al., 2014). Against our expectation, our analyses revealed the hippocampus to be involved in both, encoding threat cues and uncertain threat contexts in observational threat learning, a seemingly contradictory finding to the proposed differential role in firsthand threat learning (Marschner et al., 2008; Alvarez et al., 2011), but

see (Hur et al., 2020; Cornwell et al., 2025). In our study the hippocampus reflected the direct comparison between cue and context in predictable vs. unpredictable conditions (i.e., the threat cue-prominence, as delivered subsequently rated in the expression phase) already during observation (FWE trendwise significant cluster). This role of the hippocampus in observational threat learning might be driven by an inherent aspect of observation, which is the uncertainty of firsthand outcomes for the participants. Hence, the hippocampal involvement during observational learning might reflect threat surveillance for own firsthand outcomes, rather than only temporal predictions for the demonstrator. We found that the threat information was resolved in the left anterior hippocampus, which is in line with the functional topography of the human hippocampus, where the L1 segment is associated with fear and conditioning and strongly connected to the limbic system (Robinson et al., 2015). The hippocampus's brief activation to predictable cues on the other hand took place in the left posterior portion, an area primarily associated with spatial perception but with strong functional links to the left IFG involved in semantic encoding, a plausible role during learning cued threat contingencies (Robinson et al., 2015). In line with previous research employing direct learning (Shankman et al., 2014; Geng et al., 2018; Radoman et al., 2021) the anterior insula was involved during observation of uncertain threat anticipation (i.e., unpredictable context onsets). Furthermore, the anterior insula was involved in resolving both contextual and cue-related threat information during the expression phase. These findings extend previous work employing firsthand threat learning , which fits the finding that the insular cortex has been highlighted as a highly connected hub in threat-learning (Wheelock et al., 2014) that computes personal affects in uncertain threat-situations (Radoman et al., 2021). In conclusion our data provide evidence that observational learning of predictable and uncertain threats is resolved in areas comparable to direct learning. In line with assumptions from direct learning (Hur et al., 2020), our data suggests that the neural systems involved in threat processing react to certain and uncertain threats with a difference in degree but not in kind. Previous research has highlighted the interplay of amygdala and hippocampus in the formation of complex emotional memories guiding our reactions to threat (Cooper et al., 2024).

It has been suggested early on to accounts for learning dynamics during the acquisition of fear conditioning, i.e. dynamic rather than rigid neural responses to threat information (Quirk et al., 1997; Buchel et al., 1998a; Marschner et al., 2008). Our study enables the comparison between a simple, predictable learning condition (conditioning (cued threat) and an

unpredictable condition in which aversive outcomes are embedded in a rich but arbitrary environment (contextual threat). Consistent with previous findings (Marschner et al., 2008), we observe a linear decrease in bilateral amygdala activation towards predictable cues, while responses to unpredictable cues increase over time. This pattern persisted in the expression phase: predictable cues briefly activate the right amygdala, whereas unpredictable cues elicit sustained and increasing right amygdala activity. Similarly, the left hippocampus showed sustained activation in response to unpredictable cues. Interestingly, this explanation based on classical learning-theory, can contribute to the explanation of the interaction contrasts of cue prominence as well. During observation, the right anterior insula fades to activate to the easily resolved predictable cue and unpredictable context onset, whose meaning is more easily absorbed than v.v. For the expression phase a similar pattern can be observed in the right amygdala. It has been argued that the amygdala (Marschner et al., 2008) as well as the anterior hippocampus (Strange et al., 1999) activate to novel information that has to be integrated. Our data fits this assumption well, with a limited amygdala response to predictable threat stimuli and a dually sustained (across length of individual trial & across trials) anterior hippocampal activation to unpredictable threats. We suggest that the predictable condition lead to rapid learning and quick resolution of prediction error, while unpredictability maintains prediction error throughout (e.g. as modelled by: Rescorla et al., 1972).

We found that the left amygdala and anterior insula were activated during the observation of pain in others, which is in line with previous studies showing both, faces in pain, and depicting noxious stimulations of others' extremities (Jauniaux et al., 2019). Interestingly, we found differences in neural responses to others' pain, based on the learning condition: We found higher hemodynamic responses in the anterior insular cortex and the amygdala to observation of others' pain in the simpler learning condition (i.e. predictable condition), as compared to the unpredictable condition, where observed pain was not informative to learn threat signals (Lamm et al., 2011; Jauniaux et al., 2019). In line with this idea is our result that the observation of predictable pain, as compared to unpredictable pain, revealed neural responses in the right hippocampus that might reflect the integration of the observed pain into the learned concept. Previous research has described aberrations in vicarious stress processing to be linked to PTSD (Wesarg-Menzel et al., 2025), highlighting the importance to better understand the neural mechanisms when observed pain is integrated and when it is ignored.

The original NPU-task used startle-probes to assess whether participants learned to discriminate between cue and context related threat contingencies (Schmitz and Grillon, 2012) whereas we used SCR and explicit expectation queries. In this context, we define cue prominence as the difference of expectation or skin conductance measure with the cue present and at context onset. Previous research has successfully used SCR in direct NPU-paradigm (Alvarez et al., 2011; Hur et al., 2020) and observational learning (Olsson et al., 2007; Haaker et al., 2017b). Surprisingly we did not find meaningful psychophysiological reactions mirroring the explicitly given threat expectations. Potentially bad SCR data quality, which lead to a high drop-out rate in the analysis, has prevented the assessment of psychophysiological reactions in our study. Furthermore, a complex and inherently 'threatening' medical visual context in all conditions might have driven a strong condition independent SCR response. Future research should try to fill this gap, as previous research hints at robust SCR effects to observed pain and encounters of threat cues in the expression phase (Olsson et al., 2007; Haaker et al., 2017b).

5. Limitations

We established a novel paradigm and both experiments conceptually resemble each other closely but slightly differed in the rating procedure. Furthermore, the threat expectations after cue presence, i.e. safety ratings, did not reflect discernable (by condition) effects in participants. Since observational pain decline was slow, this might have prevented the end of the colored bar to serve as a predictable safety cue. Our sample size for Experiment 2 might have been small, given the signal to noise limitations of fMRI research. Our implication of physiological signals in this study is limited, since we were unable to find psychophysiological responses to observed pain and to threat cues and contexts, which might be a result of generally bad SCR data-quality.

6. Conclusion

Here, we show the behavioral effects and neural basis of observational learning in temporally predictable and unpredictable threat-situations across two experiments. We were able to show that healthy participants are able to resolve the cue and context related threat contingencies by observing others' experiences and make inferences towards threat for themselves. Our results provide the neural basis for vicarious learning of cued and sustained threats, to build a basis to understand anxiety and fear, in humans as socially connected individuals. We were able to show that learning processes related to temporal certainty of threats closely mirror those from

firsthand learning. On a neural level, our findings provide two novel perspectives, one that extends the neural mechanisms recruited to learn uncertain threat contingencies, and the second suggesting that such learning changes how we respond to vicariously observed pain of others. There is a solid evidence for firsthand threat learning mechanisms being linked to anxiety (Cooper et al., 2022)and obsessive compulsive disorders (Cooper and Dunsmoor, 2021). A better understanding of how vicarious processes contribute to threat learning might aid to broadening the understanding of fear, anxiety and anxiety-related disorders.

References

Alvarez RP, Biggs A, Chen G, Pine DS, Grillon C (2008) Contextual fear conditioning in humans: cortical-hippocampal and amygdala contributions. J Neurosci 28:6211-6219.

Alvarez RP, Chen G, Bodurka J, Kaplan R, Grillon C (2011) Phasic and sustained fear in humans elicits distinct patterns of brain activity. Neuroimage 55:389-400.

Andreatta M, Glotzbach-Schoon E, Muhlberger A, Schulz SM, Wiemer J, Pauli P (2015) Initial and sustained brain responses to contextual conditioned anxiety in humans. Cortex 63:352-363.

Berger SM (1962) Conditioning through vicarious instigation. Psychological Review 69:450-466.

Blanchard RJ, Yudko EB, Rodgers RJ, Blanchard DC (1993) Defense system psychopharmacology: an ethological approach to the pharmacology of fear and anxiety. Behav Brain Res 58:155-165.

Buchel C, Holmes AP, Rees G, Friston KJ (1998a) Characterizing stimulus-response functions using nonlinear regressors in parametric fMRI experiments. Neuroimage 8:140-148.

Buchel C, Morris J, Dolan RJ, Friston KJ (1998b) Brain systems mediating aversive conditioning: an event-related fMRI study. Neuron 20:947-957.

Cooper SE, Dunsmoor JE (2021) Fear conditioning and extinction in obsessive-compulsive disorder: A systematic review. Neurosci Biobehav Rev 129:75-94.

Cooper SE, Hennings AC, Bibb SA, Lewis-Peacock JA, Dunsmoor JE (2024) Semantic structures facilitate threat memory integration throughout the medial temporal lobe and medial prefrontal cortex. Curr Biol 34:3522-3536 e3525.

Cooper SE, van Dis EAM, Hagenaars MA, Krypotos AM, Nemeroff CB, Lissek S, Engelhard IM, Dunsmoor JE (2022) A meta-analysis of conditioned fear generalization in anxiety-related disorders. Neuropsychopharmacology 47:1652-1661.

Cornwell BR, Didier PR, Grogans SE, Anderson AS, Islam S, Kim HC, Kuhn M, Tillman RM, Hur J, Scott ZS, Fox AS, DeYoung KA, Smith JF, Shackman AJ (2025) A Shared Threat-Anticipation Circuit Is Dynamically Engaged at Different Moments by Certain and Uncertain Threat. J Neurosci 45.

Davis M, Walker DL, Miles L, Grillon C (2010) Phasic vs sustained fear in rats and humans: role of the extended amygdala in fear vs anxiety. Neuropsychopharmacology 35:105-135.

Figel B, Brinkmann L, Buff C, Heitmann CY, Hofmann D, Bruchmann M, Becker MPI, Herrmann MJ, Straube T (2019) Phasic amygdala and BNST activation during the anticipation of temporally unpredictable social observation in social anxiety disorder patients. Neuroimage Clin 22:101735.

Geng H, Wang Y, Gu R, Luo YJ, Xu P, Huang Y, Li X (2018) Altered brain activation and connectivity during anticipation of uncertain threat in trait anxiety. Hum Brain Mapp 39:3898-3914.

Haaker J, Yi J, Petrovic P, Olsson A (2017a) Endogenous opioids regulate social threat learning in humans. Nat Commun 8:15495.

Haaker J, Golkar A, Selbing I, Olsson A (2017b) Assessment of social transmission of threats in humans using observational fear conditioning. Nat Protoc 12:1378-1386.

Herrmann MJ, Boehme S, Becker MP, Tupak SV, Guhn A, Schmidt B, Brinkmann L, Straube T (2016) Phasic and sustained brain responses in the amygdala and the bed nucleus of the stria terminalis during threat anticipation. Hum Brain Mapp 37:1091-1102.

Hur J, Smith JF, DeYoung KA, Anderson AS, Kuang J, Kim HC, Tillman RM, Kuhn M, Fox AS, Shackman AJ (2020) Anxiety and the Neurobiology of Temporally Uncertain Threat Anticipation. J Neurosci 40:7949-7964.

Jauniaux J, Khatibi A, Rainville P, Jackson PL (2019) A meta-analysis of neuroimaging studies on pain empathy: investigating the role of visual information and observers' perspective. Soc Cogn Affect Neurosci 14:789-813.

Knobloch S, Jansen T, Haaker J (2024) nemo - fMRI. In.

Lamm C, Decety J, Singer T (2011) Meta-analytic evidence for common and distinct neural networks associated with directly experienced pain and empathy for pain. Neuroimage 54:2492-2502.

Lindstrom B, Haaker J, Olsson A (2018) A common neural network differentially mediates direct and social fear learning. Neuroimage 167:121-129.

Marschner A, Kalisch R, Vervliet B, Vansteenwegen D, Buchel C (2008) Dissociable roles for the hippocampus and the amygdala in human cued versus context fear conditioning. J Neurosci 28:9030-9036.

Naaz F, Knight LK, Depue BE (2019) Explicit and Ambiguous Threat Processing: Functionally Dissociable Roles of the Amygdala and Bed Nucleus of the Stria Terminalis. J Cogn Neurosci 31:543-559.

Olsson A, Phelps EA (2004) Learned fear of "unseen" faces after Pavlovian, observational, and instructed fear. Psychol Sci 15:822-828.

Olsson A, Nearing KI, Phelps EA (2007) Learning fears by observing others: the neural systems of social fear transmission. Soc Cogn Affect Neurosci 2:3-11.

Olsson A, Knapska E, Lindstrom B (2020) The neural and computational systems of social learning. Nat Rev Neurosci 21:197-212.

Quirk GJ, Repa C, LeDoux JE (1995) Fear conditioning enhances short-latency auditory responses of lateral amygdala neurons: parallel recordings in the freely behaving rat. Neuron 15:1029-1039.

Quirk GJ, Armony JL, LeDoux JE (1997) Fear conditioning enhances different temporal components of tone-evoked spike trains in auditory cortex and lateral amygdala. Neuron 19:613-624.

Radoman M, Lieberman L, Jimmy J, Gorka SM (2021) Shared and unique neural circuitry underlying temporally unpredictable threat and reward processing. Soc Cogn Affect Neurosci 16:370-382.

Rescorla RA, Wagner AR, Black AH, Prokasy WF (1972) A theory of Pavlovian conditioning: Variations in the effectiveness of reinforcement and nonreinforcement. In: Classical conditioning II: Current research and theory, pp 64-99: Appleton-Century-Crofts.

Robinson JL, Barron DS, Kirby LA, Bottenhorn KL, Hill AC, Murphy JE, Katz JS, Salibi N, Eickhoff SB, Fox PT (2015) Neurofunctional topography of the human hippocampus. Hum Brain Mapp 36:5018-5037.

Schmitz A, Grillon C (2012) Assessing fear and anxiety in humans using the threat of predictable and unpredictable aversive events (the NPU-threat test). Nat Protoc 7:527-532.

Shankman SA, Gorka SM, Nelson BD, Fitzgerald DA, Phan KL, O'Daly O (2014) Anterior insula responds to temporally unpredictable aversiveness: an fMRI study. Neuroreport 25:596-600.

Siminski N, Bohme S, Zeller JBM, Becker MPI, Bruchmann M, Hofmann D, Breuer F, Muhlberger A, Schiele MA, Weber H, Schartner C, Deckert J, Pauli P, Reif A, Domschke K, Straube T, Herrmann MJ (2021) BNST and amygdala activation to threat: Effects of temporal predictability and threat mode. Behav Brain Res 396:112883.

Spielberger CD, Gorsuch RL, Lushene RE (1970) STAI manual for the Stait-Trait-Anxiety Inventory (Consulting Psycholo gist, Palo Alto, CA).

Strange BA, Fletcher PC, Henson RN, Friston KJ, Dolan RJ (1999) Segregating the functions of human hippocampus. Proc Natl Acad Sci U S A 96:4034-4039.

Vachon DD, Lynam DR (2016) Fixing the Problem With Empathy: Development and Validation of the Affective and Cognitive Measure of Empathy. Assessment 23:135-149.

Vaughan KB, Lanzetta JT (1980) Vicarious instigation and conditioning of facial expressive and autonomic responses to a model's expressive display of pain. J Pers Soc Psychol 38:909-923.

Wesarg-Menzel C, Gallistl M, Niconchuk M, Engert V (2025) Adding to the burden: the tendency to resonate with others' stress is linked to higher PTSD symptom severity in individuals with war-related trauma. Transl Psychiatry 15:331.

Wheelock MD, Sreenivasan KR, Wood KH, Ver Hoef LW, Deshpande G, Knight DC (2014) Threat-related learning relies on distinct dorsal prefrontal cortex network connectivity. Neuroimage 102 Pt 2:904-912.

Tables and table legends

Table 1. Sample characteristics Experiment 1

Characteristics	Descriptives
Age (mean ± SD)	25.28 ± 3.65
Self-identified Gender	
Male, n	6
Female, n	14
Diverse, n	0
Highest Degree in Education	
Secondary School Diploma, n	2
High School Diploma, n	8
University Degree, n	8
Medical Background	
Yes, n	7
No, n	10

Table 1 legend. Table 1 reports the sample characteristics of the participants of Experiment 1. We report age (mean ± standard deviation), self identified gender, education and the binary variable medical background. Participants reported a medical background when they worked or studied in medicine or related fields like e.g. nursing.

Table 2. Sample characteristics Experiment 2

Characteristics	Descriptives
Age (mean ± SD)	27.3 ± 6.14
Self-identified Gender	
Male, n	13
Female, n	9
Diverse, n	1
Highest Degree in Education	
Secondary School Diploma, n	3
High School Diploma, n	12
University Degree, n	8
Medical Background	
Yes, n	5
No, n	18
Questionnaires	
STAI – State (mean ± SD)	33.6 ± 7.9
STAI – Trait (mean ± SD)	32.2 ± 7.3
ACME – Cognitive Empathy (mean ± SD)	27.2 ± 8.4
ACME – Affective Resonance (mean ± SD)	20.7 ± 8.9
ACME – Affective Dissonance (mean ± SD)	20.8 ± 11.4

Table 2 legend. Table 2 reports the sample characteristics of the participants of Experiment 2. We report age (mean ± standard deviation), self identified gender, education and the binary variable medical background. Participants reported a medical background when they worked or studied in medicine or related fields like e.g. nursing. Furthermore, we report the computed variables from the STAI and ACME questionnaires. Mean and standard deviation are reported.

Table 3. Experiment 1: Main effect repeated measurement ANOVA. Threat Expectation

Cases	Sum of Squares	df	Mean Square	F	p	η^2_p
Within Subjects Effects						
Condition	8.592	2	4.296	15.175	<.001	0.444
Residuals	10.758	38	0.283			
Cue/Context	21.931	1	21.931	62.033	< .001	0.766
Residuals	6.717	19	0.354			
Condition X Cue/Context	2.455	2	1.228	9.383	< .001	0.331
Residuals	4.972	38	0.131			

Table 3 legend. Table 3 reports the detailed results of the behavioral effect (threat expectation) rmANOVA (3x2: Condition: P, U, N; Timepoint: cue, context) of Experiment 1. We report sum of squares, degrees of freedom, mean square, F-values, p and an estimation of the effect sizes (partial η^2) for the main effects of condition and timepoint and the interaction effect.

Table 4. Experiment 1: Paired-sample t-tests. Learned cue-prominence after observation phase.

Variable 1	Variable 2	df	T	p	p Holm	Cohen's d
Cue-Prominence P	Cue-Prominence N	19	3.994	.00078	.00234	0.893
Cue-Prominence U	Cue-Prominence N	19	2.449	.024	.048	0.548
Cue-Prominence P	Cue-Prominence U	19	1.997	.06	.06	0.447

Table 4 legend. Table 4 reports the posthoc paired-sample t-tests conducted to analyze the significant interaction effect of the rmANOVA in Experiment 1. We compare the learned cue-prominence between all three conditions. Degrees of freedom, T, p, p corrected for multiple comparisons (Bonferroni-Holms) and an estimation of effect size (Cohen's d) are reported.

Table 5. Experiment 1: Behavioral outcome measures

Variable	Descriptives
Cue-Prominence P (mean ± SD)	117.4 ± 63.4
Cue-Prominence U (mean ± SD)	91.1 ± 65.1
Cue-Prominence N (mean ± SD)	48.0 ± 63.6
Pain-rating P (mean ± SD)	51.1 ± 19.9
Pain-rating U (mean ± SD)	49.3 ± 21.3

Table 5 legend. Table 5 reports the descriptive results of Experiment 1. We report the calculated cue-prominence for each condition (P, U, N) and the mean pain-ratings for P and U. Mean values and standard deviations are reported.

Table 6. Experiment 2: Behavioral outcome measures

Variable	Descriptives
Initial Cue-Prominence P (mean ± SD)	55.7 ± 79.6
Initial Cue-Prominence U (mean ± SD)	31.6 ± 55.9
Initial Cue-Prominence N (mean ± SD)	48.2 ± 62.6
Cue-Prominence P (mean ± SD)	82.8 ± 60.8
Cue-Prominence U (mean ± SD)	54.7 ± 56.8
Cue-Prominence N (mean ± SD)	23.5 ± 47.9
Pain-rating P (mean ± SD)	62.6 ± 20.2
Pain-rating U (mean ± SD)	66.5 ± 21.9

Table 6 legend. Table 6 reports the descriptive results of Experiment 1. We report the calculated cue-prominence for each condition (P, U, N) before (initial cue-prominence) and after learning and the mean pain-ratings for P and U. Mean values and standard deviations are reported.

Table 7. Experiment 2: Main effect repeated measurement ANOVA. Threat Expectation

Cases	Sum of Squares	df	Mean Square	F	p	η^2_p
Within Subjects Effects						
Condition	9.729[a]	2[a]	4.865[a]	22.642[a]	<.001[a]	0.507
Residuals	9.453	44	0.215			
Cue/Context	9.926	1	9.926	32.291	< .001	0.595
Residuals	6.762	22	0.307			
Condition X Cue/Context	2.022	2	1.011	13.158	< .001	0.374
Residuals	3.381	44	0.077			

Table 7 legend. Table 7 reports the detailed results of the behavioral effect (threat expectation) rmANOVA (3x2: Condition: P, U, N; Timepoint: cue, context) of Experiment 2. We report sum of squares, degrees of freedom, mean square, F-values, p and an estimation of the effect sizes (partial η^2). [a] points at the violation of the assumption of sphericity (Mauchly's test, $p < .05$).

Table 8. Experiment 2: Paired-sample t-tests. Learned cue-prominence after observation phase.

Variable 1	Variable 2	df	T	p	p Holm	Cohen's d
Learned cue-prominence P	Learned cue-prominence N	22	4.443	.0002	.0006	.926
Learned cue-prominence U	Learned cue-prominence N	22	2.814	.01	.02	.587
Learned cue-prominence P	Learned cue-prominence U	22	2.808	.01	.01	.586

Table 8 legend. Table 8 reports the posthoc paired-sample t-tests conducted to analyze the significant interaction effect of the rmANOVA in Experiment 2. We compare the learned cue-prominence between all three conditions. Degrees of freedom, T, p, p corrected for multiple comparisons (Bonferroni-Holms) and an estimation of effect size (Cohen's d) are reported.

Table 9. Experiment 2: Paired-sample t-tests. Initial cue-prominence before observation phase.

Variable 1	Variable 2	df	T	p	p Holm
Initial cue-prominence P	Initial cue-prominence N	22	0.943	.356	.356
Initial cue-prominence U	Initial cue-prominence N	22	-2.443	.023	.069
Initial cue-prominence P	Initial cue-prominence U	22	2.066	.052	.104

Table 9 legend. Table 9 reports the paired-sample t-tests conducted to analyze the cue-prominence previous to the observational learning phase in Experiment 2. We compare the learned cue-prominence between all three conditions. Degrees of freedom, T, p and p corrected for multiple comparisons (Bonferroni-Holms) are reported.

Figure legends

Figure 1: Experimental Design and Behavioral Results.

a) gives an overview of the condition design. Each condition is revealed through the moving slider, unpredictable and predictable threat, thus, can be anticipated at each condition onset. The lightning symbols depict possible positions of thermal stimulation and pain-expression. b) depicts raincloud plots of the mean threat expectation in the expression phase for context and cue of Experiment 1 & 2.

Figure 2: Observation Phase Pain.

a)-f) depict the contrast P & U > N.

a) shows a 80x80 zoom in coronary view of the left amygdala cluster. b) depicts a full volume sagittal view of the same cluster. c) shows diagrams of the peak-voxel ß-estimates of the left amygdala cluster. The respective cluster is highlighted with a red circle in a) and b).

d) shows a 80x80 zoom in coronary view of the left insula cluster. e) depicts a full volume sagittal view of the same cluster. f) shows diagrams of the peak-voxel ß-estimates of the left insula cluster. The respective cluster is highlighted with a red circle in d) and e).

g) – i) depict the contrast P > U.

g) shows a 80x80 zoom in coronary view of the right hippocampus cluster. g) depicts a full volume sagittal view of the same cluster. i) shows diagrams of the peak-voxel ß-estimates of the right hippocampus cluster. The respective cluster is highlighted with a red circle in g) and h).

Figure 3: Observation Phase: Context

a)-c) depict the contrast U > N of the context-onset.

a) shows a 80x80 zoom in coronary view of the left insula cluster. b) depicts a full volume sagittal view of the same cluster. c) shows diagrams of the peak-voxel ß-estimates of the left insula cluster. The respective cluster is highlighted with a red circle in a) and b).

d) – e) depict the contrast U > P of the sustained context activity.

d) shows a 80x80 zoom in coronary view of the right amygdala cluster. e) depicts a full volume sagittal view of the same cluster. f) shows diagrams of the peak-voxel ß-estimates of the right amygdala cluster. The respective cluster is highlighted with a red circle in d) and e).

Figure 4: Observation Phase: Cue

a)-c) depict the contrast P > N of the cue.

a) shows a 80x80 zoom in coronary view of the left hippocampus cluster. b) depicts a full volume sagittal view of the same cluster. c) shows diagrams of the peak-voxel ß-estimates of the left hippocampus cluster. The respective cluster is highlighted with a red circle in a) and b).

Figure 5: Cue Prominence

a)-c) depict the cue-prominence contrast (context: U > P, cue: P > U) of the observation phase. Note that this cluster only trends significance in FWE correction (p = 0.056).
a) shows a 80x80 zoom in coronary view of the left hippocampus cluster. b) depicts a full volume sagittal view of the same cluster. c) shows diagrams of the peak-voxel ß-estimates of the left hippocampus cluster. The respective cluster is highlighted with a red circle in a) and b).
d) – e) depict the cue-prominence contrast (context: U > P, cue: P > U) of the expression phase. d) shows a 80x80 zoom in coronary view of the right insula cluster. e) depicts a full volume sagittal view of the same cluster. f) shows diagrams of the peak-voxel ß-estimates of the right insula cluster. The respective cluster is highlighted with a red circle in d) and e).
Note: light shaded bars in both plots of the beta estimates c) and f) represent the estimates for the respective context-onsets, dark shaded bars represent the estimates for the respective cue.

Figure 6: tMod cue and context

a)-c) depict the linearly decreasing contrast P > U of the cue in the observation phase.
a) shows a 80x80 zoom in coronary view of the bilateral amygdala clusters. b) depicts a full volume sagittal view of the same clusters. c) shows diagrams of the peak-voxel ß-estimates of both amygdala clusters. The respective clusters are highlighted with red circles in a) and b).
d)-e) depict the linearly decreasing contrast P > U of the cue in the expression phase.
d) shows a 80x80 zoom in coronary view of the right amygdala cluster. e) depicts a full volume sagittal view of the same cluster. f) shows diagrams of the peak-voxel ß-estimates of the right amygdala cluster. The respective cluster is highlighted with a red circle in d) and e).
g) – i) depict the linearly decreasing contrast P > U of the sustained context activity in the expression phase.
g) shows a 80x80 zoom in coronary view of the left hippocampus cluster. g) depicts a full volume sagittal view of the same cluster. i) shows diagrams of the peak-voxel ß-estimates of the left hippocampus cluster. The respective cluster is highlighted with a red circle in g) and h).

Figure 7: tMod cue-prominence.

a)-c) depict the linearly decreasing interaction contrast of the cue-prominence in the observation phase.

a) shows a 80x80 zoom in coronary view of the right insula cluster. b) depicts a full volume sagittal view of the same cluster. c) shows diagrams of the peak-voxel ß-estimates of the right insula cluster. The respective cluster is highlighted with a red circle in a) and b).

d)-e) depict the linearly decreasing interaction contrast of the cue-prominence in the expression phase.

d) shows a 80x80 zoom in coronary view of the right amygdala cluster. e) depicts a full volume sagittal view of the same cluster. f) shows diagrams of the peak-voxel ß-estimates of the right amygdala cluster. The respective cluster is highlighted with a red circle in d) and e).

Note: light shaded bars in both plots of the beta estimates c) and f) represent the estimates for the respective context-onsets, dark shaded bars represent the estimates for the respective cue.

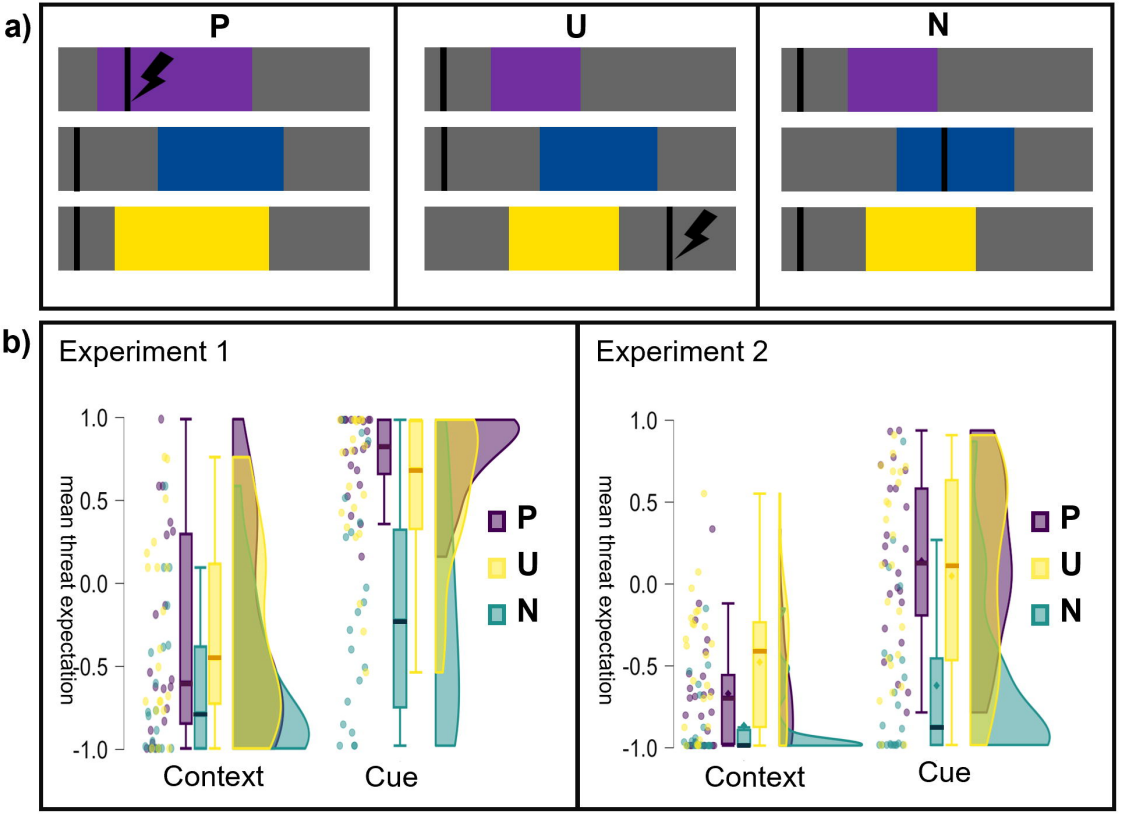
a)
P
U
N
b)
Experiment 1
Experiment 2
mean threat expectation
1.0
0.5
0.0
-0.5
-1.0
Context
Cue
P
U
N

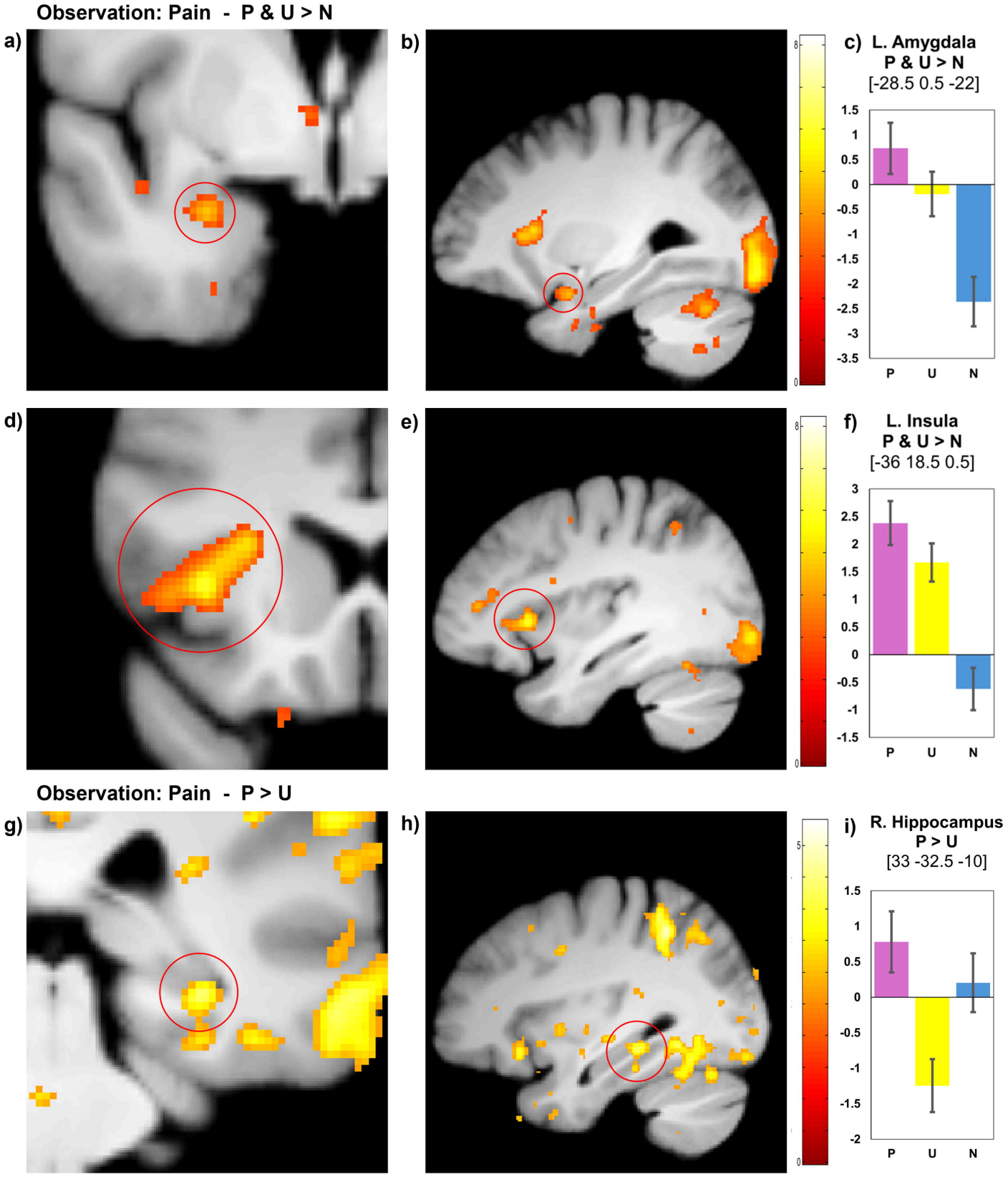
Observation: Pain - P & U > N
a)
b)
c) L. Amygdala
P & U > N
[-28.5 0.5 -22]
1.5
1
0.5
0
-0.5
-1
-1.5
-2
-2.5
-3
-3.5
P
U
N
d)
e)
f) L. Insula
P & U > N
[-36 18.5 0.5]
3
2.5
2
1.5
1
0.5
0
-0.5
-1
-1.5
P
U
N
Observation: Pain - P > U
g)
h)
i) R. Hippocampus
P > U
[33 -32.5 -10]
1.5
1
0.5
0
-0.5
-1
-1.5
-2
P
U
N

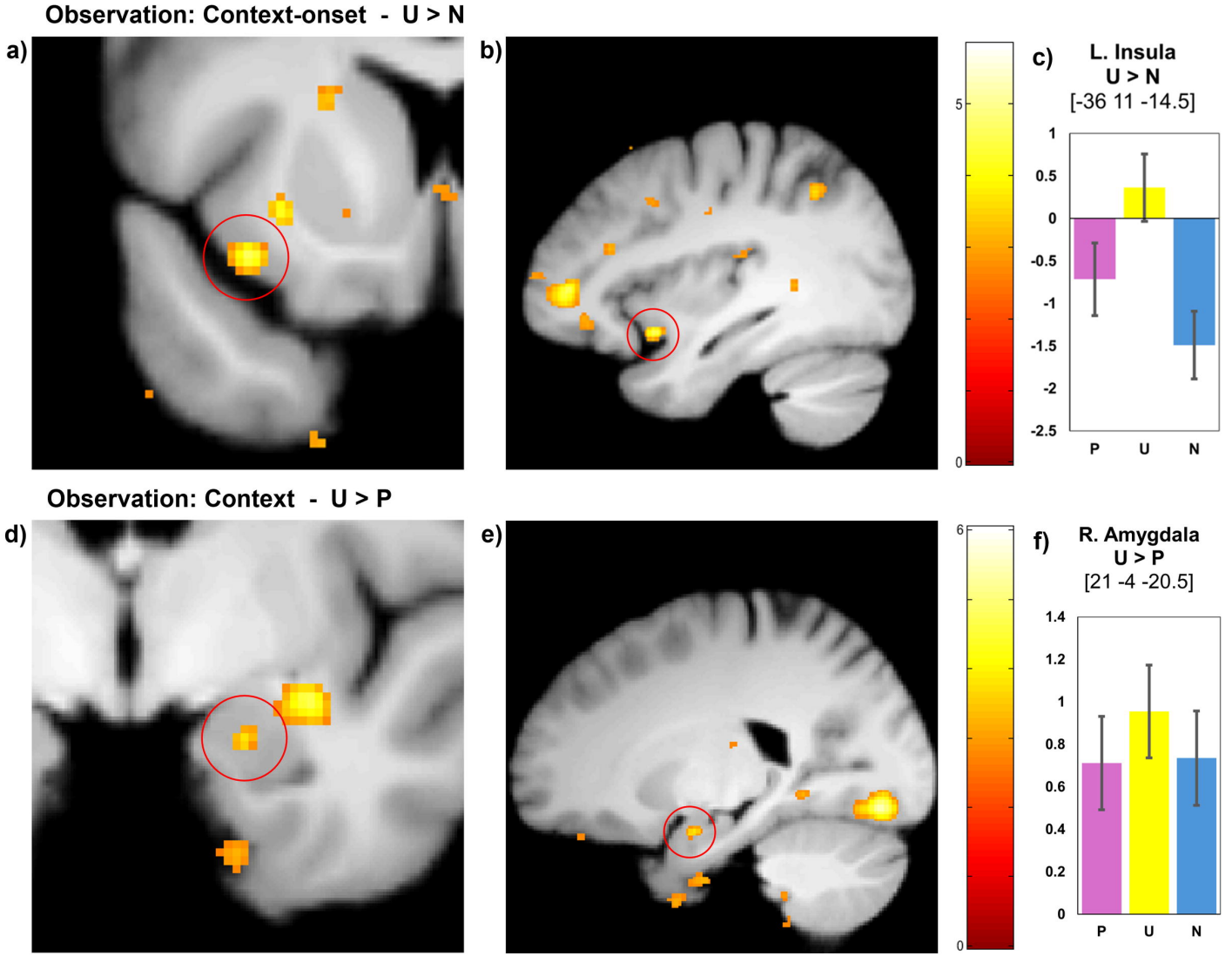
Observation: Context-onset - U > N
a)
b)
5
0
c)
L. Insula
U > N
[-36 11 -14.5]
1
0.5
0
-0.5
-1
-1.5
-2
-2.5
P
U
N
Observation: Context - U > P
d)
e)
6
0
f)
R. Amygdala
U > P
[21 -4 -20.5]
1.4
1.2
1
0.8
0.6
0.4
0.2
0
P
U
N

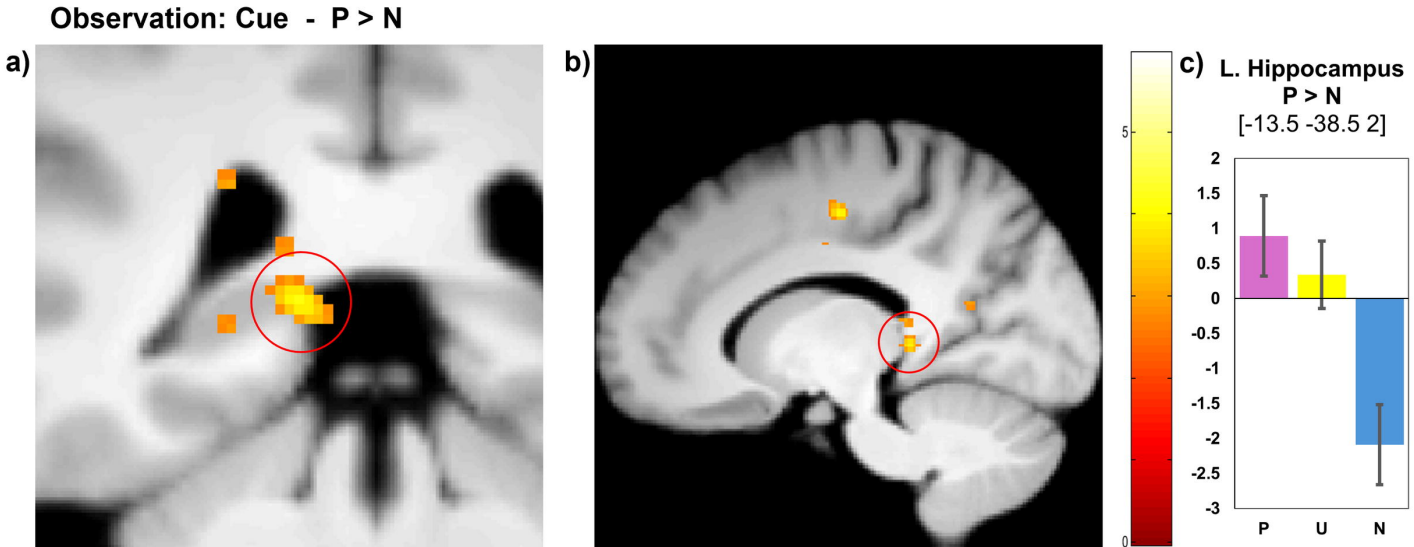
Observation: Cue - P > N
a)
b)
c)
L. Hippocampus
P > N
[-13.5 -38.5 2]
5
0
2
1.5
1
0.5
0
-0.5
-1
-1.5
-2
-2.5
-3
P
U
N

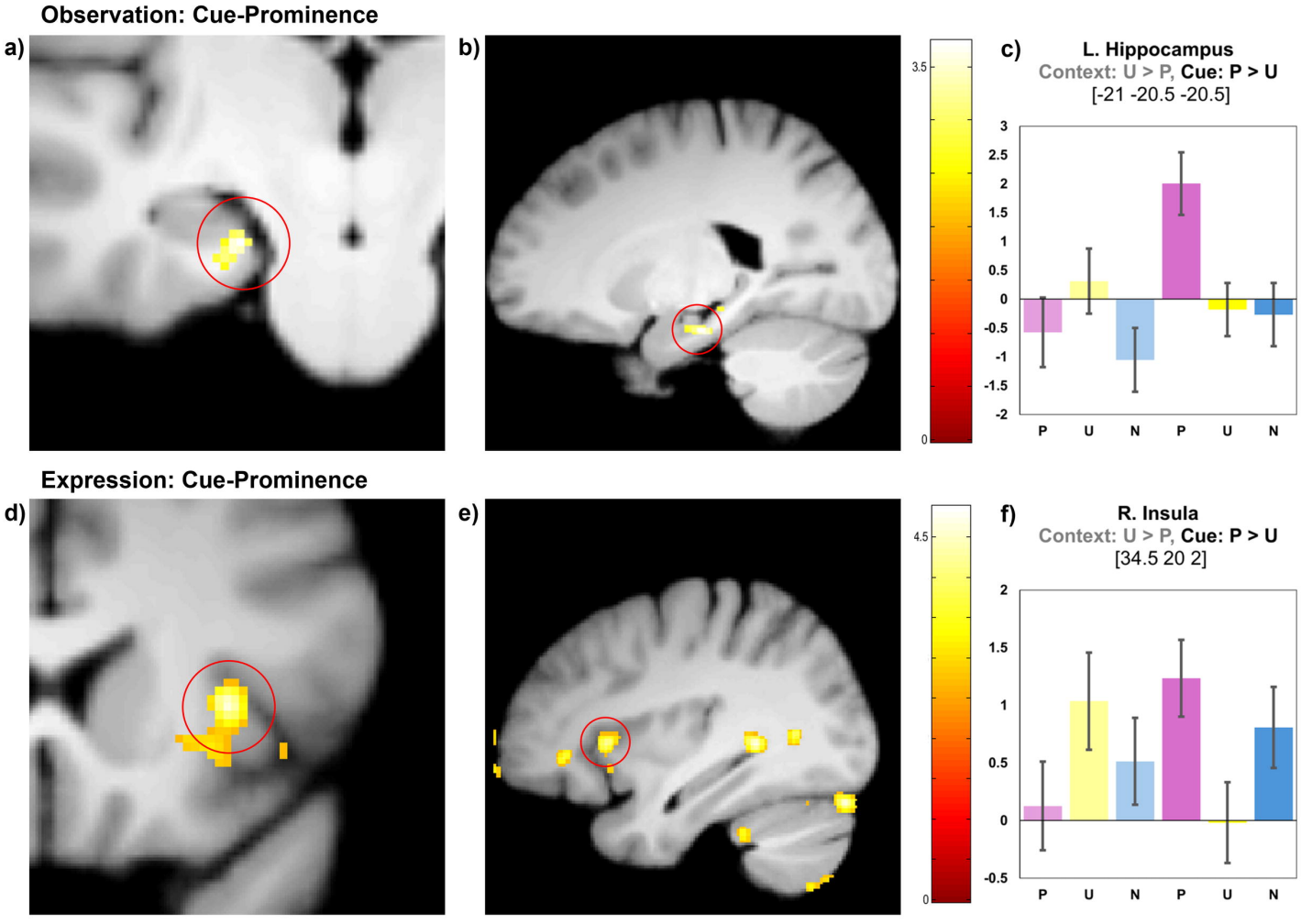
Observation: Cue-Prominence
a)
b)
3.5
0
c)
L. Hippocampus
Context: U > P, Cue: P > U
[-21 -20.5 -20.5]
3
2.5
2
1.5
1
0.5
0
-0.5
-1
-1.5
-2
P
U
N
P
U
N
Expression: Cue-Prominence
d)
e)
4.5
0
f)
R. Insula
Context: U > P, Cue: P > U
[34.5 20 2]
2
1.5
1
0.5
0
-0.5
P
U
N
P
U
N

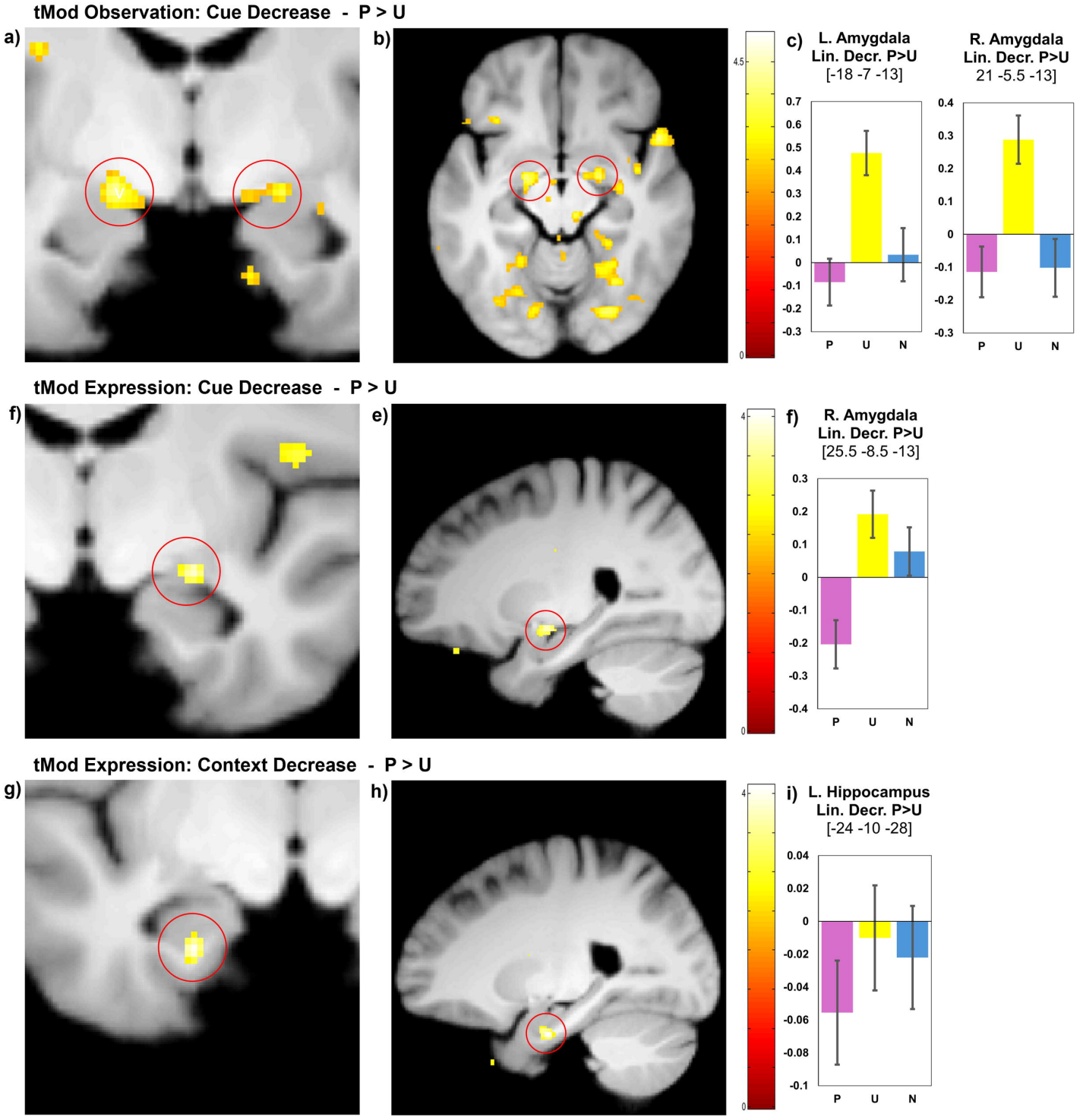
tMod Observation: Cue Decrease - P > U
a)
b)
c)
L. Amygdala
Lin. Decr. P>U
[-18 -7 -13]
R. Amygdala
Lin. Decr. P>U
21 -5.5 -13]
P
U
N
tMod Expression: Cue Decrease - P > U
f)
e)
f)
R. Amygdala
Lin. Decr. P>U
[25.5 -8.5 -13]
tMod Expression: Context Decrease - P > U
g)
h)
i)
L. Hippocampus
Lin. Decr. P>U
[-24 -10 -28]

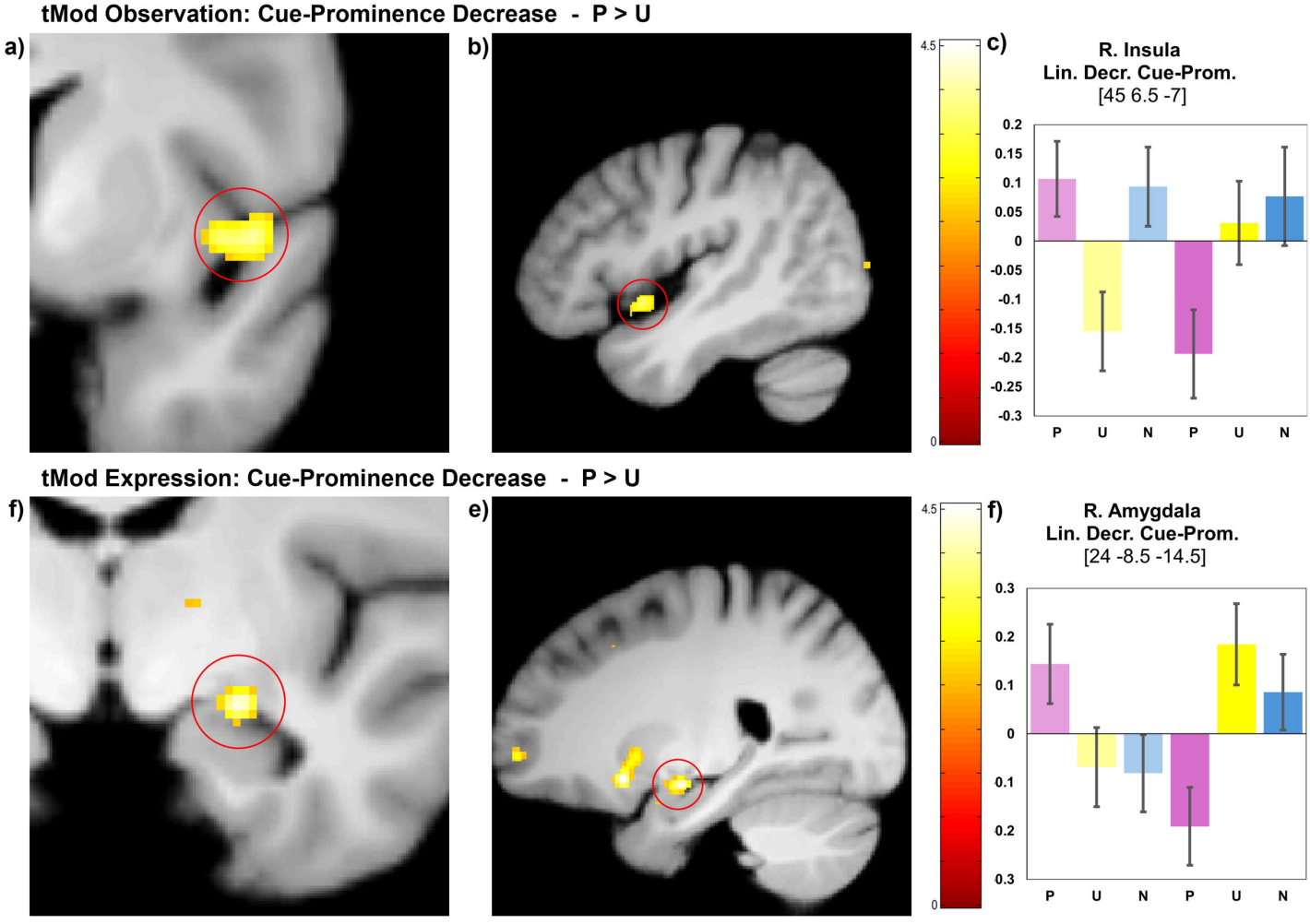
tMod Observation: Cue-Prominence Decrease - P > U
a)
b)
4.5
0
c)
R. Insula
Lin. Decr. Cue-Prom.
[45 6.5 -7]
0.2
0.15
0.1
0.05
0
-0.05
-0.1
-0.15
-0.2
-0.25
-0.3
P
U
N
P
U
N
tMod Expression: Cue-Prominence Decrease - P > U
f)
e)
4.5
0
f)
R. Amygdala
Lin. Decr. Cue-Prom.
[24 -8.5 -14.5]
0.3
0.2
0.1
0
-0.1
-0.2
-0.3
P
U
N
P
U
N